Quantification of Biomass of the Marsh Grass *Spartina alterniflora* Loisel Using Landsat Thematic Mapper Imagery

M. F. Gross
College of Marine Studies, University of Delaware, Newark, DE 19716
M. A. Hardisky
Biology Department, University of Scranton, Scranton, PA 18510
V. Klemas
College of Marine Studies, University of Delaware, Newark, DE 19716
P. L. Wolf
Biology Department, Lebanon Valley College, Annville, PA 17003

ABSTRACT: A Landsat Thematic Mapper image was used to quantify and map the distribution of live aerial biomass of the dominant grass *Spartina alterniflora* Loisel in a Delaware salt marsh. Total *S. alterniflora* live aerial biomass for the marsh was estimated from satellite-gathered radiance data to be 1.70×10^9g dry weight (gdw) distributed over 580 ha, for a mean of 294 gdw/m^2 (one standard deviation of the mean = 76 gdw/m^2). Such biomass estimates were within 13 percent of those derived from ground-gathered radiance and harvest data.

INTRODUCTION

MUCH RECENT RESEARCH has been focused on attempting to understand global biogeochemical cycling and to construct budgets of various chemical substances and elements (Abelson, 1986; Badhwar *et al.*, 1986; Bartlett, 1984; Bates *et al.*, 1986, Harriss *et al.*, 1985; Lashof, 1986; Matthews and Fung, 1986; Steudler and Peterson, 1984). The success of such efforts will depend in large part on the ability to obtain large-scale, accurate measurements of numerous variables that vary spatially and temporally (e.g., sea surface temperature, concentration of atmospheric gases, vegetation biomass, and productivity). The only practical way of gathering such measurements is to use remote sensing. Tucker *et al.* (1985, 1986) were the first to publish continental or global-scale maps of greenness or biomass from satellite data. They used data from NOAA AVHRR (Advanced Very High Resolution Radiometer) satellites that have a spatial resolution of only 1 km or 4 km, but image every point on the surface of the earth daily. While such global estimates, derived from coarse spatial resolution imagery, are very important in themselves, our understanding of observed global trends and why they are occurring can be improved by studying the biomass dynamics of selected individual plant populations or communities. This is best accomplished using satellites with spatial resolution sufficient to allow one to monitor changes that are occurring on a small spatial scale. Both the Landsat Thematic Mapper (TM) and the French satellite SPOT (Système Probatoire d'Observation de la Terre) have spatial resolutions (30 m and 20 m, respectively) that are well-suited for this purpose.

Salt marshes are generally thought to be among the most productive naturally occurring plant communities and to play a major role in global biogeochemical cycling (Bartlett, 1984). Bartlett (1976, 1979) determined that green biomass of wetland grasses was strongly correlated with the near infrared/red reflectance ratio. Bartlett and Klemas (1980) compared salt marsh vegetation biomass estimated from Landsat MSS data to biomass estimated from a limited number of harvested samples and found good agreement between the two data sources. Their results suggested that satellite data would be useful for estimating marsh biomass. Hardisky (1982, 1984) developed regression equations to predict biomass from spectral data collected using hand-held radiometers simulating Landsat TM bands, 3, 4, and 5. These equations were used to obtain remote sensing estimates of net aerial primary productivity (NAPP) of *Spartina alterniflora* Loisel, the dominant salt marsh plant along the U.S. east coast (Reimold, 1977), that differed by only 10 percent from harvest estimates (Hardisky *et al.*, 1984). This paper reports on the use of a TM image to quantify the distribution of *S. alterniflora* live aerial biomass in a Delaware salt marsh.

MATERIALS & METHODS

FIELD WORK

During mid-May and early June 1985, four plots 70 m by 70 m in size were established in the Great Marsh near Lewes, Delaware (Figure 1). These particular sites were selected because they were spatially homogeneous areas of *S. alterniflora* located in different parts of the marsh. The plots were established at least 30 m from major creeks and away from areas dominated by other vegetation types to ensure that the corresponding pixels on TM imagery would include primarily *S. alterniflora*. In each plot, stakes were placed at 10 m intervals in a grid pattern. In August, the exact location of these plots was recorded based on color infrared photographs and distances from major landscape features so that the plots could be located on the TM image.

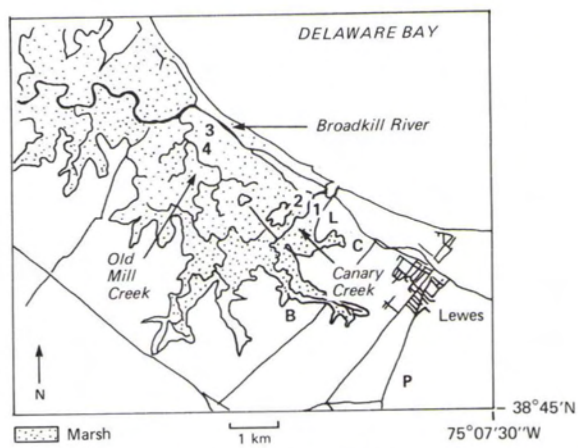

FIG. 1. Location of the four 70-m by 70-m *S. alterniflora* plots (numbered 1 to 4) and the four SSGTs (L = Lawn, C = Corn Field, B = Bare Field, and P = Pea Field).

0099-1112/87/5311–1577$02.25/0

The day preceding the 20 June 1985 Landsat overpass, several large (at least 70 m by 70 m) homogenous non-marsh targets, hereafter referred to as satellite-synchronous ground targets, or SSTGs, were chosen. The SSGTs were a pea field, a corn field, the University of Delaware Cannon Laboratory lawn, and a bare field of dry soil, all located within 5 km of the Great Marsh (Figure 1). These sites were chosen because they were large enough to be identifiable on satellite imagery without being composed of mixed pixels, were close to the marsh being studied, and were spectrally different from each other. The morning of 20 June was cloudless, and Landsat 5 was scheduled to pass over the Lewes area at approximately 1110 Eastern Daylight Savings Time (EDST). Beginning at about 1100, three to 15 radiance measurements were collected from each SSGT, as were two to four measurements of radiance from a Halon-coated panel. The Halon panel was assumed to be Lambertian. Although this is not true, the exact deviation of the Halon panel's reflectance characteristics from those of a Lambertian surface was not known, so no factors to correct for its imperfect Lambertian characteristics were applied. These measurements were collected as quickly as possible in order to obtain the measurements under solar and atmospheric conditions very similar to those at the time of the overpass. The SSGT measurements were made by two teams of investigators, each possessing a NASA GSFC Mark-II handheld radiometer (Tucker *et al.*, 1981) with filters matching TM bands 3 (0.63 to 0.69 μm), 4 (0.76 to 0.90 μm), and 5 (1.55 to 1.75 μm), and a Halon-coated panel (Butner *et al.*, 1984; Schutt *et al.*, 1984). Ground-gathered TM band 5 data were not used in the experiment. The field-of-view of the radiometer was 24°, and the radiometer was held at a height such that the ground area sensed was equal to 0.25 m^2. Dividing target radiance values by the panel radiance values in the corresponding bands yielded reflectance. The purpose of collecting data from these sites was to formulate equations relating reflectance as measured on the ground to radiance as measured by satellite, thereby accounting for atmospheric alteration of upwelling radiance. The marsh could not be used for this purpose because it is too spectrally uniform.

Between 1200 and 1400 on 20 June and 1100 and 1400 on 21 June, radiance data were collected from *S. alterniflora* canopies in each of the four 70m by 70m plots in the Great Marsh. Because one TM pixel covers a ground area of approximately 30 m by 30 m, or 900 m^2, each 4900 m^2-plot covered an area the size of about five and one-half TM pixels. One measurement was collected every 25 m^2 within each plot, for a total of 196 by 4, or 784 *S. alterniflora* radiance measurements. These measurements were made systematically by sampling the center of each of the 196 25 m^2 areas comprising a plot. One measurement of radiance from the Halon panel was taken after every 28 measurements of *S. alterniflora* radiance. The *S. alterniflora* radiance data were converted to reflectance values in TM bands 3 and 4. The canopy corresponding to every thirteenth *S. alterniflora* radiance measurement was marked with a labeled stake immediately following the collection of the radiance data. After all of the radiance data had been gathered, the aboveground vegetation within a 0.25 m^2-area centered around each stake was harvested. A representative subsample (30 to 40 percent by wet weight) of each harvested sample was selected for processing. The subsample was sorted into live leaves, live stems, and dead tissue, and each component was dried to 60°C to constant weight and then weighed.

Collecting so many radiance measurements in the marsh was an attempt to adequately sample the natural variability in each of the four plots so that the ground radiance data would be representative of each plot and could be compared to satellite radiance data. In contrast to the radiance data gathered from the SSGTs, the marsh radiance data were collected for several hours on two different days. Consequently, the elevation of the sun above the horizon varied considerably during the measurement period. Reflectance from marsh grasses, particularly at red wavelengths (TM band 3), is dependent on solar angle (M.F. Gross, unpublished data, 1987). This, in turn, causes the Normalized Difference Vegetation Index (VI; [TM4 reflectance − TM3 reflectance]/[TM4 reflectance + TM3 reflectance]), which is used to estimate biomass from reflectance data, to vary as a function of solar angle. In order to compare the ground-based data from the marsh to those collected from the satellite, the marsh reflectance data were converted to what they would have been had they all been collected at the solar elevation angle prevailing at 1110 EDST on 20 June (61.7°), the time of the satellite overpass. The algorithms used for this transformation to predicted values were developed from radiance data collected on 25 and 30 June every one-half hour between 900 and 1700 from *S. alterniflora* canopies similar to those present within the four marsh test plots. these were the dates closest to the overpass date for which data could be collected throughout the day to quantify the effects of solar angle variation on reflectance.

For the harvested samples, *S. alterniflora* reflectance data, adjusted to 1110 EDST predicted values, were plotted in the form of a VI against live aerial biomass. From these data, an equation to predict *S. alterniflora* live biomass (in grams dry weight/m^2 [gdw/m^2]) from the VI was developed based on the reduced major axis (RMA) (Curran and Hay, 1986).

TM Image Analysis • Image Rectification

An Earth Resources Data Analysis System (ERDAS) was used to analyze bands 1 to 5 of the TM image. ERDAS Version 7.0, 7.1, and 7.2 software, in addition to University of Delaware-developed ERDAS-compatible software, was employed. Careful examination of the water portions of the image revealed the presence of horizontal stripes in TM band 4. The radiance values of pixels from adjacent sets of 17 rows varied by two to three digital numbers (DNs) out of the range of 256 DNs. Striping in TM bands 1 through 3 and 5 was less than one DN and, therefore, considered to be insignificant. In TM band 4, three DNs were subtracted from the sets of rows with the high DNs in order to lessen the striping effect.

Raw Landsat data are not referenced to any map coordinate system. To facilitate future use of the Landsat data with other data types, the "destriped" data were rectified to a Universal Transverse Mercator (UTM) grid by rotation and pixel resampling. Pixels were resampled to a 30-m by 30-m size. The transformation to a UTM grid was accomplished using a cubic convolution algorithm.

TM Image Analysis • Classification

Following image rectification, a study area corresponding to the wetlands portion of the Old Mill Creek and Canary Creek drainage basins was defined. A supervised classification of this part of the image was performed, using a maximum likelihood classification algorithm to assign all pixels in the image to one of ten surface-cover/land-use classes. To verify the accuracy of the classification, the class to which each of 1,000 of the 14,780 pixels in the study area was assigned by the computer algorithm was compared to its "true" class. The true class was determined from field observations and from aerial photographs. Measures of accuracy employed were Short's Mapping Accuracy Index (MAI), User's Accuracy, and Producer's Accuracy (Rosenfield and Fitzpatrick-Lins, 1986; Story and Congalton, 1986). User's accuracy is heavily influenced by errors of commission (assignment of pixels not truly belonging to the class in question to that class), while producer's accuracy is a measure of errors of omission (assignment of pixels that belong to the class in question to a different class). Short's MAI is influenced by both omission and commission errors and is, thus, generally the most conservative of the three.

TM Image Analysis • Comparison of Image and Ground-Measured Spectral Data

The pixels comprising the SSGTs and the four *S. alterniflora* plots were located on the rectified, destriped image, and the

DNs corresponding to each of these pixels were obtained. For TM bands 3 and 4, the ground-measured reflectance values for the SSGTs were plotted against their corresponding DNs. Two equations based on the RMA were then formulated: one to convert TM band 3 radiance values as measured by the satellite to TM band 3 reflectance as measured on the ground, and one to similarly convert TM band 4 DNs to TM band 4 ground-equivalent reflectance.

To evaluate the validity of these equations, they were used to convert the DNs for the pixels representing the four *S. alterniflora* plots to reflectance and then to the VI. These VIs were compared to the mean VI for each plot calculated from the 196 ground-based reflectance measurements (following adjustment of these measurements to their 1110 EDST predicted values).

The equations to convert DNs to reflectance values served as input for a University of Delaware-developed program that converts DNs from TM bands 3 and 4 of an entire image to reflectance, and then converts these reflectance values to the VI. This permits the creation of a one-band image composed solely of the VI. These VI values are, however, in DN form because ERDAS can only display integers. A look-up table was then created to relate the integer DNs, which represent real number VIs, to their corresponding real number VIs and live aerial *S. alterniflora* biomass values. To compute the live aerial biomass of only the *S. alterniflora* areas, it was necessary to "black out" or mask the VI values for all pixels not classified as *S. alterniflora*. The result of this procedure was an image showing the VI for all *S. alterniflora* pixels in the study area. Based on the look-up table, biomass values were then assigned to the VI image to derive an image displaying *S. alterniflora* live aerial biomass.

RESULTS

Plotting the adjusted (to 1110 EDST predicted values) VIs versus biomass for the harvested *S. alterniflora* samples, and then calculating the RMA, yielded and equation to predict live aerial biomass from the VIs (Figure 2).

The number of pixels assigned to each of the surface-cover/land-use classes chosen for use in classifying the image is listed in Table 1. Six of these classes (*S. alterniflora*, *Typha/Scirpus*, *Distichlis/S. patens*, Broadleaf/Brackish, *Phragmites australis*, and *Iva Baccharis*) are composed of marsh vegetation. According to the classification produced by the computer algorithm, 40 percent of the study area was *S. alterniflora*. The next largest classes were Trees (24 percent) and Broadleaf/Brackish (11 percent).

The matrix comparing user and computer algorithm-assigned classes appears in Table 2. The classification algorithm placed 386 pixels into the *S. alterniflora* class, whereas we placed 423 pixels into the same class. This suggests that the computer algorithm underestimated the true number of *S. alterniflora* pixels

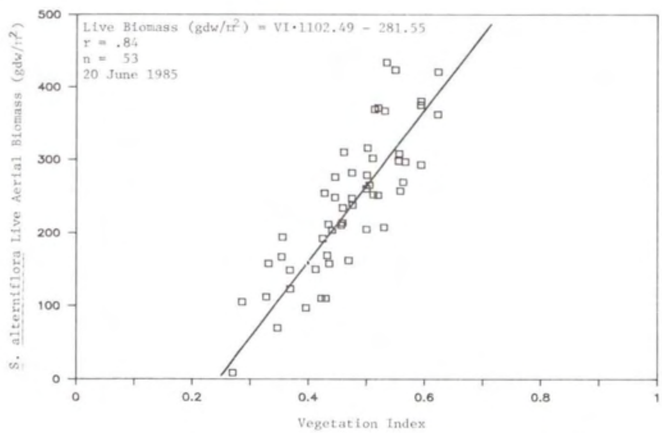

FIG. 2. Live aerial *S. alterniflora* biomass versus the VI (adjusted to predicted values at a solar angle of 61.7°).

TABLE 1. DISTRIBUTION OF STUDY AREA PIXELS AMONG CLASSES AS DETERMINED BY THE MAXIMUM LIKELIHOOD CLASSIFICATION ALGORITHM.

Class	Number of Pixels	Percent	Hectares
Spartina alterniflora	5,897	39.9	531
Typha/Scirpus	279	1.9	25
Distichlis/S. patens	1,013	6.8	91
Trees	3,587	24.3	323
Broadleaf/Brackish Marsh	1,648	11.2	148
Phragmites australis	140	1.0	13
Iva/Baccharis	756	5.1	68
Water 1	253	1.7	23
Water 2	37	0.2	3
Soil/Urban	1,170	7.9	105
	14,780	100.0	1,330

by about 10 percent. Table 3 lists the outcome of applying the three methods of assessing accuracy to this matrix. Comparison of user's accuracy with producer's accuracy indicates the relative severity of omission and commission errors for each class. The accuracy assessment measures all indicate that the *S. alterniflora* class, which contained the most pixels, was very successfully classified. *S. alterniflora* pixels were, in fact, more accurately classified than pixels in any other class (based on Short's MAI). Both omission and commission errors were low.

TM IMAGE ANALYSIS • COMPARISON OF IMAGE AND GROUND-MEASURED SPECTRAL DATA

Graphs of the mean SSGT reflectance values and the corresponding mean TM DNs are shown in Figure 3 (for TM band 3) and Figure 4 (for TM band 4). The RMA lines are shown, along with the equations defining the lines. These equations were employed to convert the radiance values in bands 3 and 4 on the TM image to reflectance. The reflectance values were then transformed into the VI. The real number VI values had to be converted to integers between zero and 255 for ERDAS to display them. Therefore, all VI values of less than zero were set equal to a DN of zero. The remaining VI values (between zero and 1) were scaled from 1 to 250, such that each DN represented an increment of 0.004 in the VI ($250*0.004=1.0$).

To test how well the satellite-derived VIs agreed with the ground-derived VIs for the four *S. alterniflora* plots, the VIs for the five pixels representing each of the four plots were recorded, and the mean VI for each plot was calculated. A comparison of the mean satellite VI to the mean VI computed from the 196 ground-based reflectance measurements (adjusted for solar angle) appears in Table 4. Satellite and ground-based means VIs differed by less than 5 percent for each plot (not significant at $p<0.05$). For both the satellite and ground-based measurements, the mean VI was highest for Plot 1, followed by Plots 2, 4, and 3.

Each pixel represents 30 m by 30 m, or 900 m^2, which equals 0.09 ha. Multiplying the number of pixels corresponding to each DN times 900 m^2/pixel (or 0.09 ha/pixel) yielded the areal extent (m^2) covered by each biomass level listed in the look-up table (not shown). Multiplying the areal extent times the biomass level (m^2*gdw/m^2) yielded the gdw of live aerial biomass for each DN. Totaling these numbers for all DNs generated an estimate of $1.55*10^9$ gdw of live aerial *S. alterniflora* biomass distributed over 527 ha, for a mean of 294gdw/m^2 ($1.55*10^9$ g/527 ha* 1 ha/10,000 m^2). The results presented in Table 2 suggest that the number of *S. alterniflora* pixels was underestimated by about 10 percent, so a revised estimate would be $1.70*10^9$ gdw distributed over 580 ha. The mean is assumed to remain constant at 294gdw/m^2.

The look-up table permitted the breakdown of the DNs into a manageable, easily visually analyzed number of classes based on biomass. After considerable manipulation of the number and boundaries of possible classes, we arbitrarily chose to form six classes spanning 60g live aerial biomass (except for classes 1 and 6). The choice of these class boundaries facilitated visual

TABLE 2. COMPARISON OF COMPUTER ALGORITHM AND USER-ASSIGNED CLASSES OF 1,000 RANDOMLY CHOSEN PIXELS.

		User*										
		Sa	Ty	DS	Tr	BB	Ph	IB	W1	W2	SU	Total
COMPUTER ALGORITHM	Sa	376	0	4	0	0	0	1	5	0	0	386
	Ty	4	6	0	0	0	0	0	8	0	0	18
	DS	7	0	51	1	2	0	10	0	0	0	71
	Tr	0	0	0	205	4	0	0	2	0	0	211
	BB	4	1	4	47	38	4	4	8	0	0	110
	Ph	0	0	0	6	1	0	0	0	0	0	7
	IB	10	0	13	5	6	0	33	0	0	0	67
	W1	0	0	0	0	0	0	0	24	1	0	25
	W2	0	0	0	0	0	0	0	2	2	0	4
	SU	22	2	5	9	2	3	4	13	0	41	101
Total		423	9	77	273	53	7	52	62	3	41	1,000

*Sa = *S. alterniflora*; Ty = *Typha/Scirpus*; DS = *Distichlis/S. patens*; Tr = Trees; BB = Broadleaf/Brackish; Ph = *P. australis*; IB = *Iva/Baccharis*; W1 = Water 1; W2 = Water 2; SU = Soil/Urban.

TABLE 3. CLASSIFICATION ACCURACY OF THE TM IMAGE.

	Percent Correct*		
Class	User's Accuracy	Producer's Accuracy	Short's Mapping Accuracy Index
S. alterniflora	97	89	87
Typha/Scirpus	33	67	28
Distichlis/S. patens	72	66	53
Trees	97	75	74
Broadleaf/Brackish	34	72	30
Phragmites australis	0	0	0
Iva/Baccharis	49	63	38
Water 1	96	39	38
Water 2	50	67	40
Soil/Urban	41	100	41

*User's Accuracy is influenced by commission errors, Producer's Accuracy is influenced by omission errors, and Short's Mapping Accuracy Index is influenced by commission and omission errors.

TABLE 4. COMPARISON OF THE GROUND-BASED AND SATELLITE-DERIVED ESTIMATES OF MEAN VI IN THE FOUR *S. ALTERNIFLORA* PLOTS.

	VI		
Plot*	Derived from Ground-Based Measurements	Derived from Landsat TM	Percent Difference
1	0.534(0.004)	0.551(0.013)	+3.2
2	0.494(0.005)	0.492(0.002)	−0.4
3	0.396(0.005)	0.414(0.012)	+4.5
4	0.456(0.005)	0.465(0.007)	+2.0

*For each plot, the listed VIs are the mean of 196 samples for the solar angle-adjusted ground-based measurements, and the mean from five pixels for the TM data. Numbers in parentheses are one standard error of the mean. There were no significant differences between satellite and ground-derived means for any of the four plots using a t-test at the 0.05 probability level.

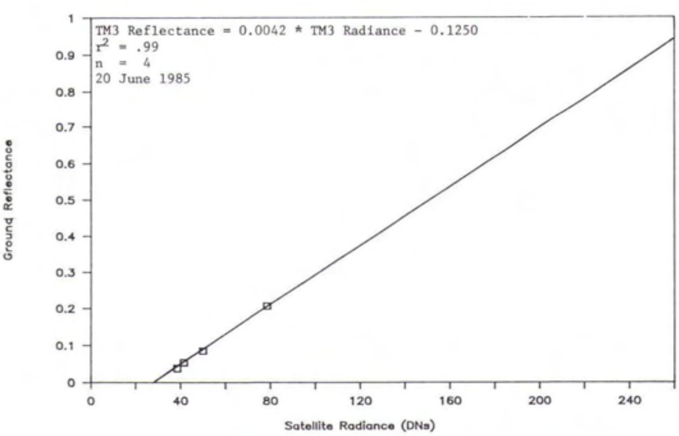

FIG. 3. Ground reflectance versus satellite radiance for the SSGTs in TM band 3.

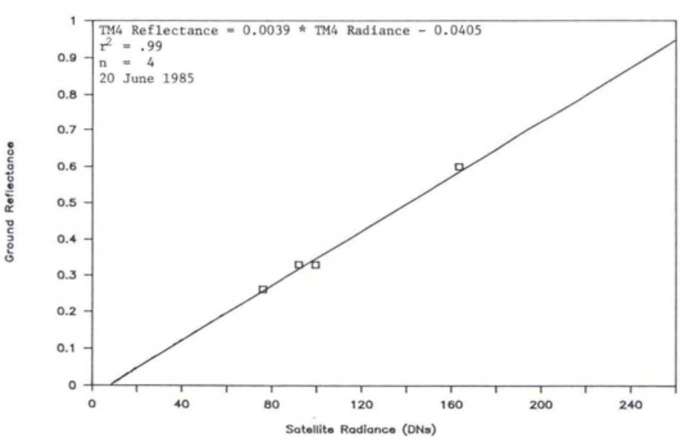

FIG. 4. Ground reflectance versus satellite radiance for the SSGTs in TM band 4.

detection of trends and patterns of biomass distribution on the image. The resulting quantified distribution of live aerial *S. alterniflora* biomass appears in Figure 5. Biomass generally seemed to be higher in the Canary Creek Marsh than in the Old Mill Creek Marsh, and was higher near the heads of the creeks, as opposed to near their mouths. Large areas of low biomass are

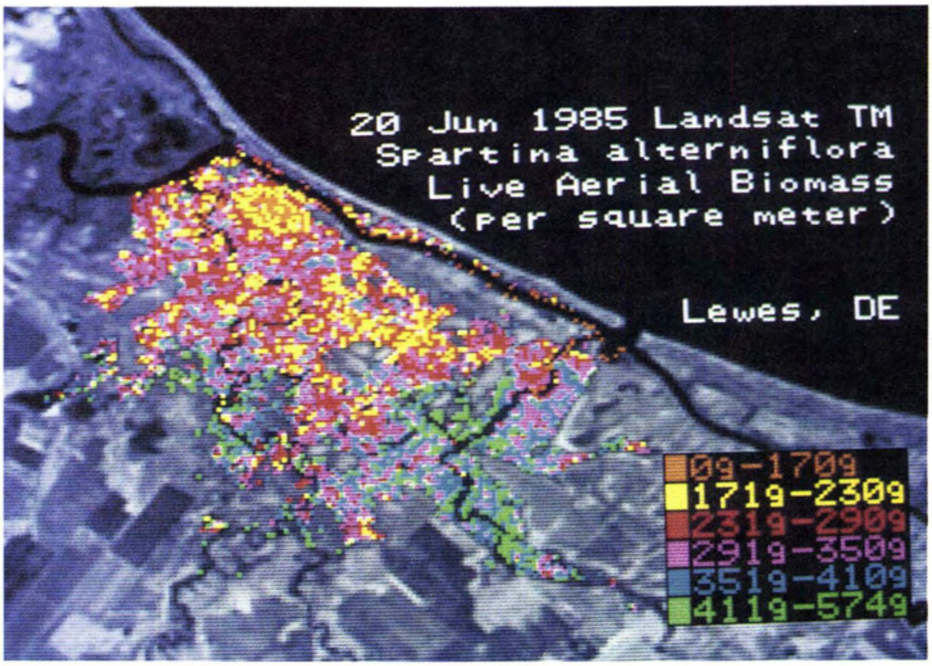

FIG. 5. Quantified distribution of live aerial *S. alterniflora* biomass in the Great Marsh, Lewes, Dele., on 20 June 1985.

evident near Plots 3 and 4. The classes, their biomass range, areal extent, and total biomass are listed in Table 5.

DISCUSSION

The relationship between radiance (and, therefore, reflectance) and satellite DNs is linear, which is a property of the Landsat TM system. Hence, in theory, only two points (two spectrally distinct SSGTs) are necessary to establish the line defining the relationship between satellite-measured radiance and ground-measured reflectance, and it is valid to extrapolate the lines shown in Figures 3 and 4 beyond the values sampled. The scatter observed in these two figures was due to the striping in the image, some spatial variability in the spectral characteristics of the SSGTs, and difficulty in identifying pixels corresponding precisely to the area sampled on the ground. Despite the excellent correlation between satellite and ground-based measurements of SSGTs in this study, formulation of the RMA lines would have been made with more confidence if it were based on eight or ten points rather than on four, as in this study.

Because the success of this study depended heavily on the accuracy of the *S. alterniflora* classification, it is fortunate that that class was the most correctly classified. Based on the most conservative accuracy assessment, the classification accuracy was a very high 87 percent. This resulted from the fact that *S. alterniflora* dominates large contiguous areas of the marsh. In many places it is pure or contains only a few individuals of *Salicornia* spp., *S. patens*, or *Distichlis spicata*. As a result of these two factors (contiguity and purity), the number of mixed pixels was minimized.

A major cause of the poor (other than for the *S. alterniflora* class) classification accuracy results (Table 3) was mixed pixels. The primary reason for the existence of many mixed pixels is that the Landsat TM's spatial resolution (30 m by 30 m) is larger than the typical areal extent of tidal creek water, *Typha/Scirpus*, *Iva/Baccharis*, *P. australis*, and *Distichlis/S. patens* zones. In other words, in many parts of the marsh, the smallest area the satellite sensor can resolve is larger than the zones of these land-cover classes. Normally, one should not attempt to distinguish classes that typically occur in patches smaller than several times the spatial resolution of the sensor. However, we chose to try to discriminate these classes to assess the type and degree of errors that would result.

The map of biomass distribution (Figure 5) shows many low biomass pixels near the point where the Broadkill River and Old Mill Creek join. Field observation in the summers of 1985 and 1986 revealed the presence of many dieback areas and salt pans (depressions mostly devoid of vascular plants) in these locations. This suggests that these areas drain poorly and that the plants in this section of the marsh are highly stressed.

The general trend in both Canary Creek Marsh and Old Mill Creek Marsh for biomass to increase as freshwater inflow increased was expected. In areas where freshwater inflow is important, salinity is lower. *S alterniflora* grows best in low or moderately saline soils (Nestler, 1977; Linthurst and Seneca, 1981). All else being equal, growth is inhibited by high salinity in the marsh areas close to the salty Delaware Bay and Broadkill River waters. One trend that was unexpected was the generally higher biomass in Canary Creek Marsh than in Old Mill Creek Marsh. This may merely reflect salinity levels. Other possible factors that may account for the higher biomass in the Canary Creek Marsh include differences in nutrient levels (particularly nitrogen) and in drainage or tidal flooding and flushing.

There are no published, verified reports of whole marsh live aerial biomass estimates available for comparison with this one.

TABLE 5. SUMMARY OF LIVE AERIAL *S. ALTERNIFLORA* BIOMASS ESTIMATED FROM THE TM IMAGE.

Level of Biomass (gdw/m^2)	Total Quantity of Biomass (gdw)	Areal Distribution (ha)
0-170	0.03×10^9	25
171-230	0.16×10^9	79
231-290	0.39×10^9	150
291-350	0.52×10^9	162
351-410	0.30×10^9	78
411-574	0.15×10^9	33
	1.55×10^9	527

Estimated area covered by *S. alterniflora* is probably underestimated by 10 percent, so revised estimates are 1.70×10^9 gdw distributed over 580ha. The mean is assumed to remain constant at $294 gdw/m^2$.

Hardisky (1984) did harvest $0.25m^2$ areas of vegetation at 24 stations within a 22-ha portion of Canary Creek Marsh every three weeks during 1981. The reported mean live biomass at his late June sampling was about $330gdw/m^2$, a quantity consistent with the results of this study.

An ultimate research objective is to obtain remote sensing estimates of whole marsh annual net aerial primary productivity (NAPP). To achieve this objective, remote sensing data must be acquired at fairly regular time intervals throughout a growing season. One way to avoid the limitations caused by the infrequency of nadir-acquired satellite data is to consider using off-nadir data. The SPOT satellite has pointable sensors, which means that coverage of a mid-latitude location can occur 12 times within a 26-day cycle, while a nadir overpass occurs only once every 26 days. A problem involved with the acquisition of data from a look angle other than nadir is that the spectral response from canopies of *S. alterniflora* (Bartlett *et al.*, 1986) and other species (Holben and Fraser, 1984; Kimes, 1984; Ranson *et al.*, 1985ab; Shibayama and Wiegand, 1985) can vary substantially with the look angle of the sensor. Thus, a correction for variation in reflectance due to look angle would have to be made, introducing additional error.

Satellites such as the AVHRR offer daily coverage of every point on Earth, in contrast to the less frequent coverage offered by Landsat and SPOT. Therefore, the chances of obtaining a clear weather overpass over a particular site are much better. However, the spatial resolution of AVHRR data is 1 km or 4 km. The 1-km by 1-km pixels are over 1,000 times the size of Landsat pixels. Consequently, AVHRR satellite data are not useful for biomass estimation when finer spatial resolution is required. The AVHRR also has a wide scan angle, so a correction for off-nadir effects must be made. Tucker *et al.* (1985) were able to successfully predict total dry biomass production in the Senegalese Sahel using AVHRR data, but the spatial resolution of their biomass estimates was limited by the satellite's 1-km resolution.

CONCLUSIONS

This study has shown that Landsat Thematic Mapper imagery can be used to accurately estimate the live aerial biomass of *S. alterniflora* throughout an entire marsh. The technique described above could be used in other areas where monospecific vegetation dominates areas several times as large as TM pixels. Because the technique has been proven, there is no need to collect large numbers of radiance measurements of the vegetation canopies (such as our collection of 784 measurements of radiance from *S. alterniflora*) for comparison with satellite DNs. Assuming equations relating the Vegetation Index (VI) to biomass, Leaf Area Index (LAI), or some other vegetation parameter were developed prior to the overpass, the only requirement for ground-truth data collection at the same time as the overpass is the collection of a number of radiance measurements from large, homogeneous targets differing spectrally from each other (SSGTs). This can be accomplished efficiently by two teams of two people, each provided with a hand-held radiometer and a reflective panel, collecting data for about one hour. Even at the current cost of a SPOT or TM image (well in excess of $1,000), this technique is a very cost-effective and practical means for deriving accurate, high spatial resolution estimates of vegetation parameters over large areas.

ACKNOWLEDGMENTS

This research was sponsored by NASA's Biospheric Research Program under Grant No. NAGW-374; by the NOAA Office of Sea Grant, Department of Commerce, under Grant No. NA85AA-D-SG033 (Project No. A/I-20); by NSF Grant No. DAR-8017836; and by the University of Delaware. The authors wish to thank H. Froozandeh for secretarial expertise, F.C. Daiber for reviewing an earlier version of the manuscript, T. Hardisky and the University of Delaware Statistics Laboratory for technical assistance, and S. Wagner and R. Rohloff for computer software development.

REFERENCES

Abelson, P.H., 1986. The international geosphere-biosphere program. *Science* 234:657.

Badhwar, G.D., R.B. MacDonald, and N.C. Mehta, 1986. Satellite-derived leaf-area-index and vegetation maps as input to global carbon cycle models—a hierarchical approach. *Int. J. Remote Sens.* 7:265–281.

Bartlett, D.S., 1976. *Variability of wetland reflectance and its effect on automatic categorization of satellite imagery*. M.S. Thesis, Univ. Delaware, Newark. 108p.

———, 1979. *Spectral reflectance of tidal wetland plant species and implications for remote sensing*. Ph.D. Dissertation, Univ. Delaware, Newark. 239p.

———, 1984. *Global Biology Research Program: Biogeochemical Processes in Wetlands*. NASA Conf. Publ. 2316, NASA, Washington, D.C. 44p.

Bartlett, D.S., and V. Klemas, 1980. Quantitative assessment of tidal wetlands using remote sensing. *Environ. Mgt.* 4:337–345.

Bartlett, D.S., R.W. Johnson, M.A. Hardisky, and V. Klemas, 1986. Assessing impacts of off-nadir observation on remote sensing of vegetation: Use of the Suits model. *Int. J. Remote Sens.* 7:247–264.

Bates, T.S., R.J. Charlson, and R.H. Gammon, 1986. Evidence for the climatic role of marine biogenic sulfur. *EOS* 67:1051 (Abstract).

Butner, C.L., J.B. Schutt, and M.C. Shai, 1984. Comparison of the reflectance characteristics of polytetrafluoroethylene and barium sulfate paints. *Appl. Opt.* 23:1139–1140.

Curran, P.J., and A.M. Hay, 1986. The importance of measurement error for certain procedures in remote sensing at optical wavelengths. *Photogrammetric Engineering and Remote Sensing* 52:229–241.

Hardisky, M.A., 1982. *The relationship between spectral radiance and aboveground biomass of* **Spartina alterniflora** *Loisel*. M.S. Thesis, Univ. Delaware, Newark. 112p.

———, 1984. *Remote sensing of aboveground biomass and annual net aerial primary productivity in tidal wetlands*. Ph.D. Dissertation, Univ. Delaware, Newark. 252p.

Hardisky, M.A., F.C. Daiber, C.T. Roman, and V. Klemas, 1984. Remote sensing of biomass and annual net aerial primary productivity of a salt marsh. *Remote Sens. Environ.* 16:91–106.

Harriss, R.C., E. Gorham, D.I. Sebacher, K.B. Bartlett, and P.A. Flebbe, 1985. Methane flux from northern peatlands. *Nature* 315:652–654.

Holben, B., and R.S. Fraser, 1984. Red and near-infrared sensor response to off-nadir viewing. *Int. J. Remote Sens.* 5:145–160.

Kimes, D.S., 1984. Modeling the directional reflectance from complete homogeneous vegetation canopies with various leaf-orientation distributions. *J. Opt. Soc. Am.* A1:725–737.

Lashof, D.A., 1986. Carbon storage in the biosphere and global climate. *EOS* 67:1052 (Abstract).

Linthurst, R.A., and E.D. Seneca, 1981. Aeration, nitrogen, and salinity as determinants of *Spartina alterniflora* Loisel. growth response. *Estuaries* 4:53–63.

Matthews, E., and I. Fung, 1986. Methane emission from wetland ecosystems. *EOS* 67:1050 (Abstract).

Nestler, J., 1977. Interstitial salinity as a cause of ecophenic variation in *Spartina alterniflora*. *Est. Coastal Mar. Sci.* 5:707–714.

Ranson, K.J., C.S.T. Daughtry, L.L. Biehl, and M.E. Bauer, 1985a. Sun-view angle effects on reflectance factors of corn canopies. *Remote Sens. Environ.* 18:147–161.

Ranson, K.J., L.L. Biehl, and M.E. Bauer, 1985b. Variation in spectral response of soybeans with respect to illumination, view and canopy geometry. *Int. J. Remote Sens.* 6:1827–1842.

Reimold, R.J., 1977. Mangals and salt marshes of eastern U.S. *Wet Coastal Ecosystems* (V.J. Chapman, ed.), Elsevier Scientific: New York pp. 157–166.

Rosenfield, G.H., and K. Fitzpatrick-Lins, 1986. A coefficient of agreement as a measure of thematic classification accuracy. *Photogrammetric Engineering and Remote Sensing* 52:223–227.

Schutt, J.B., C.M. Shai, and J.H. Henninger, 1984. Optical coatings formulations containing tetrafluoroethylene. *Appl. Opt.* 23:1138.

Shibayama, M., and C.L. Wiegand, 1985. View azimuth and zenith, and solar angle effects on wheat canopy reflectance. *Remote Sens. Environ.* 18:91–103.

Steudler, P.A., and B.J. Peterson, 1984. Contribution of gaseous sulphur from salt marshes to the global sulphur cycle. *Nature* 311:455–457.

Story, M., and R.G. Congalton, 1986. Accuracy assessment: A user's perspective. *Photogrammetric Engineering and Remote Sensing* 52:397–399.

Tucker, C.J., I.Y. Fung, C.D. Keeling, and R.H. Gammon, 1986. Relationship between atmospheric CO_2 variations and a satellite-derived vegetation index. *Nature* 319:195–199.

Tucker, C.J., W.H. Jones, W.A. Kley, and G.J. Sundstrom,1981. A three-band hand-held radiometer for field use. *Science* 211:281–283.

Tucker, C.J., C. Vanpraet, M.J. Sharman, and G. Van Ittersum, 1985. Satellite remote sensing of total herbaceous biomass production in the Senegalese Sahel: 1980–1984. *Remote Sens. Environ.* 17:233–249.

(Received 13 March 1987; accepted 29 May 1987; revised 17 June 1987)